

**International Journal of Innovative Research in Science,  
Engineering and Technology**

*(A High Impact Factor, Monthly, Peer Reviewed Journal)*

Visit: [www.ijirset.com](http://www.ijirset.com)

Vol. 8, Issue 2, February 2019

# Origin of Strong Dielectric Response in the Pseudo-Cubic BF-0.5PFN: An X-Ray Powder Diffraction Study

Jay Prakash Patel

Department of Physics Govt. Post College Musafirkhana Amethi, Uttar Pradesh, India

**ABSTRACT:** The impurity free BF-0.5PFN sample is successfully synthesized by solid state reaction route. The temperature dependence dielectric measurement was carried out to confirm the diffuse ferroelectric transition in pseudo-cubic BF-0.5PFN. The Rietveld analysis of room temperature x-ray powder diffraction pattern was carried out to confirm the room temperature crystal structure of BF-0.5PFN. The local structure refinement of x-ray powder diffraction pattern confirm the local disorder for the  $\text{Bi}^{3+}/\text{Pb}^{2+}$  and  $\text{O}^{2-}$  along the  $\langle xxz \rangle$  and  $\langle 110 \rangle$  directions from their cubic positions respectively.

## I. INTRODUCTION

$\text{BiFeO}_3$  (BF) is only known room temperature multiferroic with having highest value of ferroelectric  $T_C \sim 830$  °C [1] and antiferromagnetic  $T_N \sim 370$  °C [2-4]. The room temperature crystal structure of BF is rhombohedral with  $R\bar{3}c$  space group. The ferroelectricity in BF is due to presence of stereochemically active  $6s^2$  lone pair of Bi and their hybridization with O  $2s/2p$  atomic orbitals [5-7]. This results in the cooperative displacement of  $\text{Bi}^{3+}$  and  $\text{Fe}^{3+}$  ions along [111] direction gives rise to a ferroelectric polarization. The ferroelectric polarization  $P \sim 100$   $\mu\text{C}/\text{cm}^2$  has been reported in BF single crystal [8]. In quest of improved multiferroic properties, I have synthesized the different composition of solid solution of BF and  $\text{Pb}(\text{Fe}_{1/2}\text{Nb}_{1/2})\text{O}_3$  (PFN). I have selected BF-0.5PFN composition among different possible compositions of BF and  $\text{Pb}(\text{Fe}_{1/2}\text{Nb}_{1/2})\text{O}_3$  (PFN) solid solutions for the present study. The room temperature structure of BF-0.5PFN appears to be cubic but show non-relaxor diffuse type of dielectric response with temperature. The huge dielectric response of BF-0.5PFN could not be explained by cubic symmetry (with  $\text{Pm}\bar{3}m$  space group) because the presence of inversion symmetry. To correlate the dielectric properties of BF-0.5PFN with crystal structure, I have carried out the Rietveld analysis of x-ray diffraction data and shows that average crystal structure of BF-0.5PFN is pseudo-cubic. In this manuscript I have shown that the ferroelectric properties of BF-0.5PFN are linked with local disorder of  $\text{Bi}^{3+}/\text{Pb}^{2+}$  and  $\text{O}^{2-}$  from its ideal cubic positions.

## II. EXPERIMENTAL

BF-0.5PFN powders were synthesized by solid state reaction method. Analytical reagent grade reagents  $\text{Bi}_2\text{O}_3$  (99.5%, Himedia),  $\text{Fe}_2\text{O}_3$  (99%, Himedia),  $\text{PbCO}_3$  (99.5%) and  $\text{Nb}_2\text{O}_5$  (99.0%, Himedia) were taken as the initial raw materials. All the powders were having purity  $\geq 99\%$ . The reacting species in the stoichiometric ratio were thoroughly mixed in an agate mortar-pestle in the presence of AR grade acetone for 2-3 hours. The mixtures were then ball milled (Retsch GmbH & Rheinische, Germany) for 6 hours using zirconia jars and zirconia balls with AR grade acetone as the mixing media. After proper mixing (hand mixing and ball milling), mixture was kept at least for 12 hours to completely evaporate the acetone which was used during ball milling. The dried powder was gently collected and used for calcinations. The ball milled powder was calcined at 890 °C for 7 hours. The calcined powder was grind in to fine powders by using an agate mortar and pestle and used for the collection of x-ray diffraction patterns. The x-ray diffraction pattern was indexed by using JCPDS files. Since, there were no reflections of ingredient powders  $\text{Bi}_2\text{O}_3$ ,  $\text{Fe}_2\text{O}_3$ ,  $\text{PbCO}_3$  and  $\text{Nb}_2\text{O}_5$  present in XRD patterns it means reactions were completely taken place. Temperature

## International Journal of Innovative Research in Science, Engineering and Technology

(A High Impact Factor, Monthly, Peer Reviewed Journal)

Visit: [www.ijirset.com](http://www.ijirset.com)

Vol. 8, Issue 2, February 2019

dependent dielectric measurements were carried out using a Novocontrol (Alpha-A) high performance frequency analyzer. The laboratory x-ray measurements were carried out using an 18 kW rotating anode (Cu) based Rigaku powder diffractometer operating in the Bragg-Brentano geometry and fitted with a curved crystal monochromator in the diffraction beam. The data were collected in the  $2\theta$  range of 20 to  $120^\circ$  at a scan step of  $0.02^\circ$ .

### III. RESULTS AND DISCUSSION

**3.1 Dielectric study:** Figure 1 (a, b) depicts the temperature dependent variation of real component  $\epsilon'$  and imaginary component  $\epsilon''$  of the complex dielectric permittivity for BF-0.5PFN measured at 1 and 3 kHz frequencies. The real part of the dielectric permittivity  $\epsilon'$  shows the diffuse anomaly at  $T_m \sim 227^\circ\text{C}$ , probably due to freezing of the local electric dipoles while the imaginary part of the dielectric permittivity  $\epsilon''$  shows a peak approximately at the magnetic transition temperature  $\sim 177^\circ\text{C}$ . The local electric dipoles are induced because of certain degree of disorder in the crystalline structure. Generally, three different types of disorders are found in complex perovskite (i) disorder accompanied by variation in local electric field e.g.  $\text{Pb}(\text{Mg}_{1/3}\text{Nb}_{2/3})\text{O}_3$  (PMN) (ii) disorder accompanied by variation in local strain field e.g.  $(\text{Bi}, \text{Ba})(\text{Fe}, \text{Ti})\text{O}_3$ ,  $\text{K}\text{aTiO}_3$  and (iii) disorder accompanied by vacancies e.g. PLZT [9-12]. The disorder associated with local electric field is due to the imbalance of cationic charges at the A and B-site of the cubic perovskite while disorder due to the strain field associated with the difference in their ionic radii. In the present study, BF-0.5PFN has  $(\text{Bi}^{3+}, \text{Pb}^{2+})$  and  $(\text{Fe}^{3+}, \text{Nb}^{5+})$  ions at their A-site and B-site of the cubic perovskite. The ionic radii of  $\text{Bi}^{3+}$ ,  $\text{Pb}^{2+}$  are  $\sim 1.17 \text{ \AA}$ ,  $\sim 1.19 \text{ \AA}$  and for  $\text{Fe}^{3+}$ ,  $\text{Nb}^{5+}$  are  $\sim 0.645 \text{ \AA}$ ,  $\sim 0.74 \text{ \AA}$  respectively which are comparable for both the ionic sites. Therefore, possibilities of local disorders at the A and B-sites of the cubic perovskite due to the strain field (differences in their cationic radii), if any is negligible. However, considerable local displacement of  $\text{Bi}^{3+}/\text{Pb}^{2+}$  along  $\langle 110 \rangle$  pseudo-cubic directions of cubic may occurred due to the variation in the local electric field. This type of displacement may be understood as follows. If we consider the single unit cell of BF-0.5PFN, the ions  $\text{Fe}^{3+}/\text{Nb}^{5+}$ ,  $\text{Bi}^{3+}/\text{Pb}^{2+}$  may occupy the (0,0,0) and (0.5,0.5,0.5) positions which are the centers of the octahedron and cuboctahedron respectively. There is 25% probability to occupy the 8 cube corners positions by  $\text{Nb}^{5+}$  rest of by  $\text{Fe}^{3+}$  because BF-0.5PFN has  $\text{Fe}^{3+}/\text{Nb}^{5+}$  ratio 3. If  $\text{Nb}^{5+}$  occupy the two corner points of one of eight diagonals, the  $\text{Bi}^{3+}/\text{Pb}^{2+}$  does not get off centered because of cancellation of coulomb repulsing forces along one of  $\langle 111 \rangle$  diagonals. But if  $\text{Nb}^{5+}$  occupy the corner position along the face diagonal or end of the axial positions, these give the net displacement of  $\text{Bi}^{3+}/\text{Pb}^{2+}$  along the  $\langle 110 \rangle$  direction to valence the coulomb repulsive forces along the  $\langle 111 \rangle$  directions. Conclusively, the charge imbalance at A and B-site of the cubic perovskite gives off center displacement of  $\text{Bi}^{3+}/\text{Pb}^{2+}$  along  $\langle 110 \rangle$ . The off center displacement of  $\text{Bi}^{3+}/\text{Pb}^{2+}$  might be linked with the observed dielectric  $\epsilon''(T)$  response.

**3.2. Local structure of BF-0.5 PFN:** Fig. 2 depicts x-ray diffraction pattern for the BF-0.5PFN. The (200), (220) and (222) peaks profiles for this composition is found to be singlet. The absence of superlattice reflection with singlet peaks

profiles indicates the cubic like crystal structure for this composition. The cubic structure with space group  $\text{Pm}\bar{3}\text{m}$  was used for the Rietveld refinements of BF-0.5PFN composition. The  $\text{Bi}^{3+}/\text{Pb}^{2+}$  atom kept at Wyckoff site 1 a: (0, 0, 0),  $\text{Fe}^{3+}/\text{Nb}^{5+}$  at 1 b: (1/2, 1/2, 1/2) and  $\text{O}^{2-}$  at 3 c: (1/2, 1/2, 0). The pseudo-voigt wave function was used for the peak profile matching, while the linear interpolation method was used for the background refinement. The refinement was first carried out using isotropic thermal parameters ( $B_{iso}$ ) for all the atomic sites. Reasonably satisfactory fit was obtained ( $R_{wp} = 5.88\%$ ), but the isotropic thermal parameters have very high values  $B_{iso}(\text{Bi}/\text{Pb}) = 5.89 \text{ \AA}^2$ ,  $B_{iso}(\text{O}) = 3.53 \text{ \AA}^2$  and comparatively small value for the  $\text{Fe}^{3+}/\text{Nb}^{5+}$  atomic site. Refinement with anisotropic thermal parameters for the  $\text{Bi}^{3+}/\text{Pb}^{2+}$  and  $\text{O}^{2-}$  atoms gives slightly improved fit ( $R_{wp} = 5.83\%$ ) with  $\beta_{11} = \beta_{22} = \beta_{33} = 0.092 \text{ \AA}^2$  for the  $\text{Bi}^{3+}/\text{Pb}^{2+}$  and  $\beta_{11} = \beta_{22} = 0.070 \text{ \AA}^2 \neq \beta_{33} = 0.026 \text{ \AA}^2$  for the  $\text{O}^{2-}$  ions. The refinement results show that a high thermal displacement parameter for the  $\text{Bi}^{3+}/\text{Pb}^{2+}$  and  $\text{O}^{2-}$ , indicating off centre displacement of these ions from their cubic positions. The high values for the thermal parameters are common for the Pb-based perovskites and are well known in the literature, and are usually ascribed to local disordered displacements, which may be either dynamic or static.

## International Journal of Innovative Research in Science, Engineering and Technology

(A High Impact Factor, Monthly, Peer Reviewed Journal)

Visit: [www.ijirset.com](http://www.ijirset.com)

Vol. 8, Issue 2, February 2019

Rietveld refinement fit as shown in Fig. 3 reveal that the reflections of the type (eeo) for example (441, 522), (432, 520), (430, 500), (421), (322, 410), (531), (443, 540, 621) and (542, 630) reflections are not modeled with  $Pm\bar{3}m$  symmetry only, the calculated intensity for above reflections are lower than the observed intensity while some of others reflections for example (332), (433), (530) and (311) have calculated intensity greater than the observed intensity. In order to improve the Rietveld refinement fit, I consider the three off centre models for the  $Bi^{3+}/Pb^{2+}$  atoms from their ideal cubic position (i) 1a (0, 0, 0) site to the 6e (x, 0, 0) site with occupancy 1/6, (ii) 1a (0, 0, 0) site to the 12i (x, x, 0) site with occupancy 1/12 and (iii) 1a (0, 0, 0) site to the 8g (x, x, x) site with occupancy 1/8. I have applied commonly used procedure consisting of a series of refinements based on a particular model in which atomic displacements along particular directions were fixed but all other parameters were refined. Fig. 4(a) depicts the variation of the weighted profile ( $R_{wp}$ ) parameters with local atomic displacements in the directions  $\langle 100 \rangle$ ,  $\langle 110 \rangle$  and  $\langle 111 \rangle$ . The agreement factor ( $R_{wp}$ ) show minima for the local disorder of  $Bi^{3+}/Pb^{2+}$  in the  $\langle 100 \rangle$ ,  $\langle 110 \rangle$  and  $\langle 111 \rangle$  directions but lowest minima was found in the  $\langle 100 \rangle$  direction for  $x = 0.35 \text{ \AA}$ . Thus the local disorder of  $Bi^{3+}/Pb^{2+}$  along  $\langle 100 \rangle$  gives the better refinement ( $R_{wp} = 5.26 \%$ ) with  $B_{iso} = 2.25 \text{ \AA}^2$ . Further, the local disorder of the type  $\langle xxz \rangle$  is considered for the  $Bi^{3+}/Pb^{2+}$  atoms gives better refinement ( $R_{wp} = 5.20 \%$ ) with  $B_{iso} = 1.94 \text{ \AA}^2$ . The  $Bi^{3+}/Pb^{2+}$  displacement along  $\langle 110 \rangle$  is  $x = 0.091 \text{ \AA}$  which is very small in comparison with  $Bi^{3+}/Pb^{2+}$  displacement  $z = 0.338 \text{ \AA}$  along  $\langle 100 \rangle$  direction. The Rietveld refinement with A-site local disorder gives the acceptable values of thermal parameter for the  $Bi^{3+}/Pb^{2+}$  atoms but oxygen atom still has very high isotropic thermal parameter  $B_{iso} = 3.43 \text{ \AA}^2$ . Further,  $\langle 100 \rangle$ ,  $\langle 110 \rangle$  and  $\langle 111 \rangle$  off centre models were used for the oxygen atom. Out of the three off centre models  $\langle 100 \rangle$ ,  $\langle 110 \rangle$  and  $\langle 111 \rangle$ ,  $\langle 110 \rangle$  model gives the lowest  $R_{wp}$  with off centre displacement of  $\sim 0.2 \text{ \AA}$  as can be seen in Fig. 4(b, d), which depicts the variation of  $R_{wp}$  and  $B_{iso}$  of  $O^{2-}$  with off-center displacement along the  $\langle 110 \rangle$  directions. The application of both local disorder for the  $Bi^{3+}/Pb^{2+}$  and  $O^{2-}$  along the  $\langle xxz \rangle$  and  $\langle 110 \rangle$  directions respectively gives the lowest  $R_{wp}$  and approximately remove the mismatch between the observed and calculated profiles. The local disorder of the  $O^{2-}$  atom along the  $\langle 110 \rangle$  directions might be the reminiscent of the octahedral tilting seen in the BF-0.5PFN compositions. This type of local disorder may be called as rotational disorder and also reported in the cubic phase of the piezoelectric PZT [11].

**3.3. Correlation of Diffuse Phase Transition in BF-0.5PFN with Local Structure:** The Rietveld refinement of x-ray diffraction data proves the local displacement of the  $Bi^{3+}/Pb^{2+}$  along  $\langle xxz \rangle$  directions with  $x = 0.091 \text{ \AA}$  and  $z = 0.335 \text{ \AA}$ . The local disorder of  $Bi^{3+}/Pb^{2+}$  along  $\langle xxz \rangle$  may be considered as sum of the local disorder along the  $\langle 110 \rangle$  and  $\langle 001 \rangle$  respectively. I have already discussed in previous section the origin of the local disorder of  $Bi^{3+}/Pb^{2+}$  along  $\langle 110 \rangle$  in BF-0.5PFN. Now question is what is the origin of local disorder of  $Bi^{3+}/Pb^{2+}$  along  $\langle 001 \rangle$ ? I argue the local displacement of  $Bi^{3+}/Pb^{2+}$  along  $\langle 001 \rangle$  is due to the hybridization of  $6s^2$  lone pair orbital of  $Bi^{3+}/Pb^{2+}$  to the 2p orbitals of the neighbouring  $O^{2-}$ . In Pb based system like  $PbTiO_3$ , it is believed that the off-centering of  $Pb^{2+}$  occurs because of the softening of the short-range repulsive forces by the hybridization of the  $6s^2$  lone pair orbital of  $Pb^{2+}$  with the 2p orbitals of the oxygen ion [13]. The role of the soft mode involvement in local disorder of  $Pb^{2+}$  in well known canonical relaxor  $Pb(Mg_{1/3}Nb_{2/3})O_3$  is well established. Thus in BF-0.5PFN system the net local displacement of  $Bi^{3+}/Pb^{2+}$  by  $\langle xxz \rangle$  is resultant of the  $\langle xx0 \rangle$  local disorder because of the cationic imbalance at the A and B-site of the cubic perovskite and  $\langle 00z \rangle$  because of the softening of the short range repulsive forces by the hybridization of the  $6s^2$  lone pair orbitals of  $Bi^{3+}/Pb^{2+}$  with the 2p orbitals of  $O^{2-}$ . The occurrence of randomly oriented non-interacting polar nano clusters or polar nano-regions (PNR) in BF-0.5PFN above  $T_m$  holds key to explain the smeared  $\epsilon'$  (T) transitions. The system is in the so-called ergodic (violated paraelectric) state consisting of dynamic, randomly oriented polar nanoclusters distributed within the paraelectric matrix. In the vicinity of  $T_m$ , the system undergoes a phase transitions from the ergodic to nonergodic state consisting of static, coupled polar nanoclusters. This type of transitions gives the relaxor ferroelectric state in the  $Pb(Mg_{1/3}Nb_{2/3})O_3$  while the non-relaxor diffuse ferroelectric state in the BF-0.5PFN. In PMN-like relaxor ferroelectrics, the coupled polar nanoclusters are small enough to show relaxational freezing in the

## International Journal of Innovative Research in Science, Engineering and Technology

(A High Impact Factor, Monthly, Peer Reviewed Journal)

Visit: [www.ijirset.com](http://www.ijirset.com)

Vol. 8, Issue 2, February 2019

Curie range, leading to the frequency dependent  $T'_{\max}$  and  $T''_{\max}$  but there is no evidence for such relaxational dynamics of the coupled polar nanoclusters in BF-0.5PFN.

### IV. CONCLUSION

The results of the present study are summarized point wise as follows:

- (i) The impurity free sample of BF-0.5PFN was successfully synthesized.
- (ii) The diffuse dielectric plot confirms the ferroelectric to paraelectric transition in pseudo-cubic BF-0.5PFN composition.
- (iii) The structural analysis by using x-ray diffraction data shows average crystal structure of BF-0.5PFN is pseudo-cubic (space group  $Pm\bar{3}m$ ) with locally disorder of  $Bi^{3+}/Pb^{2+}$  and  $O^{2-}$  along  $\langle xxz \rangle$  and  $\langle 110 \rangle$  respectively.
- (iv) The presence of polar nano-regions (PNR) in BF-0.5PFN is responsible for the smeared ferroelectric transition.

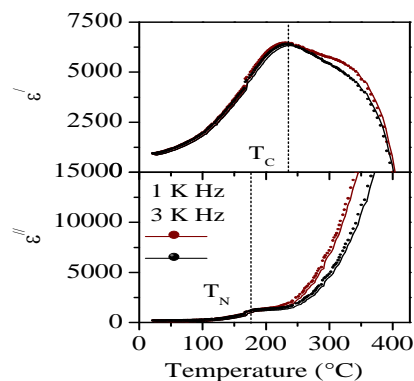


Fig. 1

# International Journal of Innovative Research in Science, Engineering and Technology

(A High Impact Factor, Monthly, Peer Reviewed Journal)

Visit: [www.ijirset.com](http://www.ijirset.com)

Vol. 8, Issue 2, February 2019

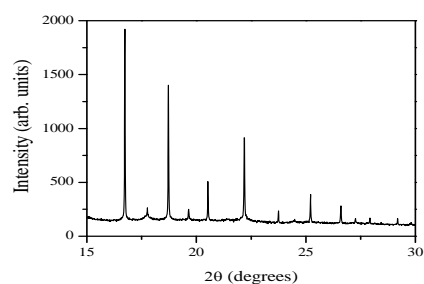


Fig. 2

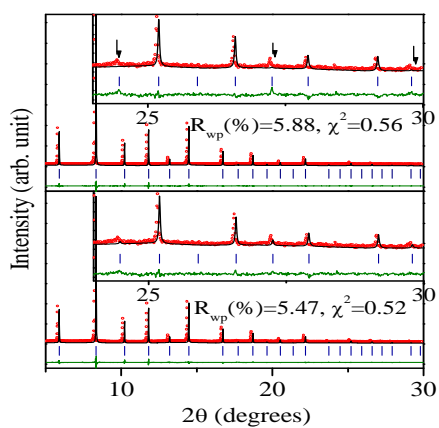


Fig. 3

## International Journal of Innovative Research in Science, Engineering and Technology

(A High Impact Factor, Monthly, Peer Reviewed Journal)

Visit: [www.ijirset.com](http://www.ijirset.com)

Vol. 8, Issue 2, February 2019

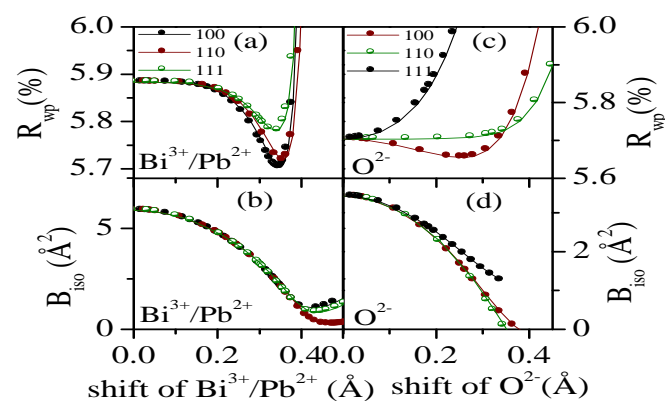


Fig. 4

### Figure Captions:

Figure 1: Temperature dependences of (a) real and (b) imaginary part of dielectric constant measured at 1 and 3.0 kHz frequencies. The vertical dotted line at maxima of real part of dielectric constant indicates the ferroelectric transition temperature while the vertical dotted line at the maxima of imaginary part of the dielectric constant indicates the paramagnetic to antiferromagnetic transition temperature.

Figure 2: The room temperature x-ray diffraction pattern for BF-0.5PFN.

Figure 3: Rietveld refinement fit of room temperature x-ray diffraction data (a) by using Cubic model (Pm-3m space group) with isotropic thermal parameters and (b) Cubic model (Pm-3m space group) with local disorders for  $\text{Bi}^{3+}/\text{Pb}^{2+}$  and  $\text{O}^{2-}$  atoms along the  $\langle 100 \rangle$ ,  $\langle 110 \rangle$  and  $\langle 111 \rangle$  directions respectively with isotropic thermal parameters. The reflections indicated by arrows and stars are of the types  $h+k+l = \text{even}$  and  $h+k+l = \text{odd}$  respectively. The dots, fitted line and horizontal line below vertical ticks are observed, calculated, and difference profiles. The vertical ticks mark the positions of the reflections.

Figure 4: Variation of weighted profile agreement factor  $R_{wp}$  with off centered- displacement of (a)  $\text{Bi}^{3+}$  and  $\text{Pb}^{2+}$  (b)  $\text{O}^{2-}$  along the pseudocubic  $\langle 100 \rangle$ ,  $\langle 110 \rangle$  and  $\langle 111 \rangle$  directions respectively. Variation of isotropic thermal parameter ( $B_{iso}$ ) with off centered displacement of (c)  $\text{Bi}^{3+}$  and  $\text{Pb}^{2+}$  (d)  $\text{O}^{2-}$  along the pseudocubic  $\langle 100 \rangle$ ,  $\langle 110 \rangle$  and  $\langle 111 \rangle$  directions respectively.

### REFERENCES

- [1] W. Kaczmarek and Z. Pajak, Solid State Commun. 17, 807(1975).
- [2] I. Sosnowaska, T. Peterlin-Neumaier, and E. Steichele, J. Phys. C 15, 4835 (1982).
- [3] A. J. Jacobson and B. E. F. Fender, J. Phys. C 8, 844(1975).
- [4] Yu. E. Roginskaya et al., Sov. Phys. JETP 23, 47(1966).

## International Journal of Innovative Research in Science, Engineering and Technology

*(A High Impact Factor, Monthly, Peer Reviewed Journal)*

Visit: [www.ijirset.com](http://www.ijirset.com)

**Vol. 8, Issue 2, February 2019**

- [5]. J.-H. Lee, H. J. Choi, D. Lee, Min G. Kim, C. W. Bark, S. Ryu, M.- A. Oak and H. M. Jang, Phys. Rev. B 82, 045113 (2010).
- [6] C. Ederer and N. A. Spaldin, Phys. Rev. B 71, 060401(R) (2005).
- [7] A. H. Hill, F. Jiao, P. G. Bruce, A. Harrison, W. Kockelmann and C. Ritter, Chem. Mater. 20, 4891(2008).
- [8] D. Lebeugle, D. Colson, A. Forget, and M. Viret, Appl. Phy. Lett. **91**, 022907(2007).
- [9] Mathan N. D., Husson E., Calvarin G., Gavarrri J. R., Hewat A. W., and Morell A., J. Phys.: Condens. Matter 3, 8159 (1991).
- [10] Dkhil B., Kiat J. M., Calvarin G, Baldinozzi G., Vkhurushev S. B. and Surad E., Phys. Rev. B 65, 024104-024111(2001).
- [11] Zhang N., Yokota H., Glazer A. M. and Thomas P. A., Acta Cryst. B67, 461-466 (2011).
- [12] Thomas N. W., Ivanov S. A., Ananta S., Tellgren R. and Rundlof H, J. Eur. Ceramic Society 19, 2667-2675(1999).
- [13] R. E. Cohen, Nature London **358**, 136 (1992)